



Light controls gene functions through alternative splicing in fungi

Yifan Li^a , Huanhong Lu^a, Degang Guo^a, Xiaoyan Li^a, Fei Qi^b , Jian Zhang^a, Reinhard Fischer^{c,1} , Qirong Shen^{a,1}, and Zhenzhong Yu^{a,1}

Edited by Jay Dunlap, Dartmouth College Geisel School of Medicine, Hanover, NH; received January 15, 2025; accepted May 23, 2025

Light controls important biological processes in fungi by regulating transcriptional gene activation. Here, we found that beyond the regulation of mRNA transcript abundance, light regulates alternative splicing (AS) in the filamentous fungi *Aspergillus nidulans*, *Trichoderma guizhouense*, and *Neurospora crassa*. Blue light-regulated AS was involved in ergothioneine biosynthesis and conidiation in *T. guizhouense*, which required the blue light receptor BLR1. Blue light activated the MAPK HOG (Sak) pathway which then transmitted the signal via the serine/threonine kinase SRK1 to the AS key regulator SRP1. SRK1 and SRP1 are important for light-induced conidiation. The light-activated HOG pathway led to an increase of the SRK1 protein level and its phosphorylation status. Phosphorylated SRK1 translocated from the cytoplasm to the nucleus to interact with SRP1, thereby regulating AS efficiency. This study unravels another level of complexity of fungal environmental sensing and responses and also first describes the entire cascade from an environmental signal to the splicing machinery.

fungi | light sensing | alternative splicing | ergothioneine biosynthesis | conidiation

Alternative splicing (AS) is important in multicellular eukaryotes, which enables a single pre-mRNA to generate multiple mRNA isoforms, thereby significantly enhancing proteome diversity and functional complexity (1–3). This process is mediated by the spliceosome, composed of ribonucleoprotein particles and numerous splicing factors (4). The spliceosome precisely recognizes and binds to intronic consensus sequences, catalyzing intron removal and exon ligation to produce mature mRNA (5). Many spliceosomal proteins are conserved between fungi and humans, and their crucial roles for AS in fungi have been demonstrated (6).

In fungi, AS was first reported in the industrial fungus *Aspergillus niger*, where two glucoamylase isoforms (G1 and G2) are generated from a single gene (7). Although AS is less frequent in fungi compared to plants and animals, it is still widespread and important (8). In the human pathogen *Cryptococcus neoformans*, each gene contains an average of 5.7 introns, and the incidence of AS is around 18.2% (9, 10). In the plant pathogen *Fusarium graminearum*, the RNA-binding protein FgRbp1 enhances the recruitment of the splicing factor FgU2AF23, thereby affecting 47% of intron-containing transcripts involved in growth, development, and virulence (11). As in higher eukaryotes, AS of a specific gene in fungi may be crucial for specific biological processes. In the plant pathogen *Ustilago maydis*, the peroxisomal targeting signal of the glyceraldehyde-3-phosphate dehydrogenase (GAPDH) resulting from AS of the *gapdh* gene is crucial for its virulence (12). In the human pathogen *Candida albicans*, the antifungal menadione exposure induces AS of the superoxide dismutase-encoding gene *sod3*, leading to reduced fungicide resistance (13). Therefore, AS is important for several fungal biological processes. It has also been shown that fungi that interact with higher eukaryotes can target the splicing machinery of the hosts. In the case of arbuscular mycorrhizal fungi, fungal SP7-like effectors interact with the plant spliceosome proteins SR45, U1-70 K, and U2AF35, resulting in plant developmental changes that correlate with AS modulation of specific genes (14).

Little is known yet about the mechanisms of how environmental signals may lead to AS in fungi. One important environmental cue is light, which is an indicator for putative stressful conditions. Hence, light regulates a wide range of physiological and morphological processes (15, 16). In the model fungus *Aspergillus nidulans*, red light represses sexual development while promoting asexual conidiation through the phytochrome FphA and the MAPK HOG (Sak) pathway (17, 18). FphA senses red light and then activates the MAPK SakA to regulate the transcriptional activation of light-responsive genes. In contrast, in the plant-beneficial fungus *Trichoderma guizhouense*, blue light is decisive for conidiation, making it a great model for studying blue light signaling. Blue light is perceived by the blue light receptor BLR1, the ortholog of the *Neurospora crassa* white collar 1 protein, and the signal transmitted through the MAPK HOG pathway to regulate gene

Significance

Light is a pivotal environmental signal that controls biological processes by regulating gene transcript abundances. This study unravels a regulatory mechanism whereby light signals regulate alternative splicing (AS) in filamentous fungi. We showed that AS regulates important fungal biological processes, illustrated in the species *Trichoderma guizhouense* in which it impacts the biosynthesis of the ergothioneine metabolite and formation of asexual spores. The research defines how an extracellular signal reaches the splicing machinery through a sensor protein and downstream signaling pathway to regulate intron splicing in fungi.

Author affiliations: ^aJiangsu Provincial Key Lab of Solid Organic Waste Utilization, Jiangsu Collaborative Innovation Center for Solid Organic Waste Resource Utilization, Educational Ministry Engineering Center of Resource-saving fertilizers, Department of Plant Nutrition and Fertilizer Science, College of Resources and Environmental Sciences, Nanjing Agricultural University, Nanjing 210095, China; ^bState Key Laboratory of Cellular Stress Biology, Department of Genetics and Developmental Biology, School of Life Sciences, Xiamen University, Xiamen 361102, China; and ^cDepartment of Microbiology, Institute for Applied Biosciences, Karlsruhe Institute of Technology-South Campus, Karlsruhe D-76131, Germany

Author contributions: Y.L., R.F., Q.S., and Z.Y. designed research; Y.L., H.L., D.G., X.L., F.Q., and J.Z. performed research; Y.L., H.L., D.G., X.L., F.Q., and J.Z. analyzed data; and Y.L., R.F., Q.S., and Z.Y. wrote the paper.

The authors declare no competing interest.

This article is a PNAS Direct Submission.

Copyright © 2025 the Author(s). Published by PNAS. This article is distributed under [Creative Commons Attribution-NonCommercial-NoDerivatives License 4.0 \(CC BY-NC-ND\)](https://creativecommons.org/licenses/by-nc-nd/4.0/).

¹To whom correspondence may be addressed. Email: reinhard.fischer@kit.edu, shenqirong@njau.edu.cn, or yuzhenzhong@njau.edu.cn.

This article contains supporting information online at <https://www.pnas.org/lookup/suppl/doi:10.1073/pnas.2500966122/-/DCSupplemental>.

Published June 27, 2025.

transcription (19). Additionally, another blue light receptor ENV1, the ortholog of *N. crassa* VIVID, represses this process to avoid an overreaction to light. While significant progress has been made in understanding how fungi respond to light at the level of transcriptional gene activation, the role of AS in regulating fungal light responses is largely unknown.

In this study, we investigated the influence of light on AS in *A. nidulans*, *T. guizhouense*, and *N. crassa* and revealed its biological functions in regulating the antioxidant ergothioneine biosynthesis and the conidiation process in *T. guizhouense*. Furthermore, we elucidated a molecular mechanism underlying light-regulated AS.

Results

Light Regulates AS in Different Filamentous Fungi. Light has been shown to control AS in plants to mediate light responses (20). Therefore, we speculated that in fungi light could regulate not only transcriptional gene activation but also AS. Light-regulated gene transcription has been well studied in *A. nidulans*, *N. crassa*, and *T. guizhouense*, with red and far-red light sensing characterized in *A. nidulans* and blue light sensing in *N. crassa* and *T. guizhouense* (15, 19). To test the above hypothesis, we investigated the influence of light exposure on AS in these species. We performed transcriptome analysis after short-term red- and far-red-light exposure of *A. nidulans* and blue light exposure of *T. guizhouense*. Significant AS events (FDR < 0.05) were identified based on the ratios of splice junction usage under specific light conditions compared to the ratios in the dark, using transcriptomic data derived from three biological replicates per condition. Each event was then categorized into one of five types—retained intron (RI), skipped exon (SE), mutually exclusive exon (MXE), alternative 5' splice site (A5SS), or alternative 3' splice site (A3SS). In *A. nidulans* wild type (WT), 107 AS events of 100 genes were regulated by red light, 78 AS events of 75 genes were regulated by far-red light, and 51 events were regulated by both red and far-red light (Fig. 1 *A* and *B* and [Dataset S1A](#) and [S1B](#)). Among these, 43 and 31 events exhibited enhanced splicing patterns under red and far-red light, respectively, while 64 and 47 events showed repressed splicing patterns under the same conditions ([Dataset S1A](#) and [S1B](#)). Similarly, in *T. guizhouense*, blue light triggered 63 AS events of 59 genes in WT, including 36 events with enhanced splicing efficiency and 27 events with repressed splicing efficiency (Fig. 1 *C* and *D* and [Dataset S1C](#)). RI was the most frequent splicing type in both fungi, with 101 red light-regulated events and 74 far-red-light-regulated events in *A. nidulans*, and 49 blue light-regulated events in *T. guizhouense* (Fig. 1 *A* and *C* and [Dataset S1A–S1C](#)). These findings indicate the capacity of different wavelengths of light to regulate AS in both fungi.

To further explore whether light regulates AS in other fungi, we analyzed the light-responsive transcriptome data of *N. crassa* from publicly available datasets, in which WT was exposed to white light for 15 (L15), 60 (L60), 120 (L120), or 240 (L240) min after 24 h of culture in the dark (21). Compared to darkness, light regulated AS in *N. crassa* in a dynamic manner, increasing from 29 events of 27 genes at L15 to 43 events of 38 genes at L60, peaking at 46 events of 44 genes at L120, and then decreasing to 23 events of 20 genes at L240 (Fig. 1 *E* and *F* and [Dataset S1D](#)). Some events were identified at multiple time points, while others were time-point specific (Fig. 1*F*). Among these, 68 events exhibited enhanced splicing patterns, while 73 events showed repressed splicing patterns ([Dataset S1D](#)). Similarly, RI was the most frequent splicing type, with 24, 29, 31, and 16 events under L15, L60, L120, and L240 conditions, respectively (Fig. 1*E* and [Dataset S1D](#)). These results reveal the dynamic regulation of AS by light in *N. crassa*.

To assess whether light-regulated AS occurs in orthologous genes across different fungi, we performed comparative analysis among *A. nidulans*, *T. guizhouense*, and *N. crassa*. The comparison between *A. nidulans* and *T. guizhouense* identified only one orthologous gene whose transcripts exhibited RI in response to light ([Dataset S1E](#)). Specifically, blue light enhanced splicing of OPB39239 transcripts in *T. guizhouense*, while far-red light-repressed splicing of its ortholog AN9179 transcripts in *A. nidulans*. The comparison between *A. nidulans* and *N. crassa* identified two orthologous genes whose transcripts exhibited RI in response to light ([Dataset S1E](#)). In detail, transcripts of NCU10853 in *N. crassa* exhibited enhanced splicing under L15, while transcripts of its ortholog AN4936 in *A. nidulans* showed repressed splicing under red and far-red light. Transcripts of the other gene, NCU03084, displayed a repressed splicing pattern under L120 and L240 in *N. crassa*, and its ortholog AN1115 exhibited a similar pattern under far-red light in *A. nidulans*. However, the comparison between *T. guizhouense* and *N. crassa* did not identify orthologous genes ([Dataset S1E](#)). These findings suggest that light-regulated AS varies across three fungal species.

Photoreceptors and the MAPK HOG (Sak) Pathway Control Light-Regulated AS in *A. nidulans* and *T. guizhouense*. To investigate the regulatory functions of photoreceptors and the MAPK HOG (Sak) pathway in light-regulated AS, we then analyzed the transcriptomes of phytochrome ($\Delta fphA$) and MAPK SakA ($\Delta sakA$) mutants of *A. nidulans*, and blue light receptor ($\Delta blr1$ and $\Delta env1$) and MAPK HOG1 ($\Delta hog1$) mutants of *T. guizhouense*. In *A. nidulans*, the number of red light-regulated events dramatically decreased in the $\Delta fphA$ (28 events) and $\Delta sakA$ (39 events) mutants (Fig. 1 *A* and *B*). A similar trend was found in far-red light, with 19 events in the $\Delta fphA$ mutant and 29 events in the $\Delta sakA$ mutant. Notably, 92.5% (99/107) red and 92.3% (72/78) far-red-light-regulated events in WT were coregulated by FphA and Saka (Fig. 1*B*). Furthermore, 78.6% (22/28) red and 89.5% (17/19) far-red-light-regulated events in the $\Delta fphA$ mutant, as well as 92.3% (36/39) red and 86.2% (25/29) far-red-light-regulated events in the $\Delta sakA$ mutant were not present in WT (Fig. 1*B*). Only 4 red and 2 far-red-light-regulated events were overlapped between $\Delta fphA$ and $\Delta sakA$ mutants. Similarly, in *T. guizhouense*, the number of blue light-regulated events decreased to 34 in the $\Delta blr1$ mutant, whereas $\Delta env1$ and $\Delta hog1$ mutants retained comparable numbers to WT, with 69 and 66 events, respectively (Fig. 1 *C* and *D*). Furthermore, 71.4% (45/63) events in WT were coregulated by BLR1 and HOG1, and 70.6% (24/34) events in $\Delta blr1$, 75.4% (52/69) events in $\Delta env1$, and 81.8% (54/66) events in $\Delta hog1$ mutants were not present in WT (Fig. 1*D*). Only 2 events were overlapped among $\Delta blr1$, $\Delta env1$, and $\Delta hog1$ mutants. These data reveal that photoreceptors and the MAPK HOG (Sak) pathway play pivotal roles in the control of light-regulated AS in both fungi.

To investigate whether photoreceptors and the MAPK HOG1 (SakA) regulate AS in the dark, we compared the ratios of splice junction usage in specific mutants to the ratios in WT under dark conditions. Compared to WT in the dark, 51 and 71 AS events were identified in $\Delta fphA$ and $\Delta sakA$ mutants of *A. nidulans*, respectively ([SI Appendix, Fig. S1](#)). Likewise, 25, 56, and 114 AS events were identified in $\Delta blr1$, $\Delta env1$, and $\Delta hog1$ mutants of *T. guizhouense*, respectively ([SI Appendix, Fig. S1](#)). These results demonstrate that even in the dark photoreceptors and the MAPK HOG1 (SakA) still play roles in regulating AS.

To validate the transcriptome data, we selected two genes from the two fungi and confirmed the AS pattern via Integrative Genomics Viewer (IGV), semiquantitative PCR (sqPCR), and intron splicing ratio analysis. Indeed, red- and far-red-light-regulated

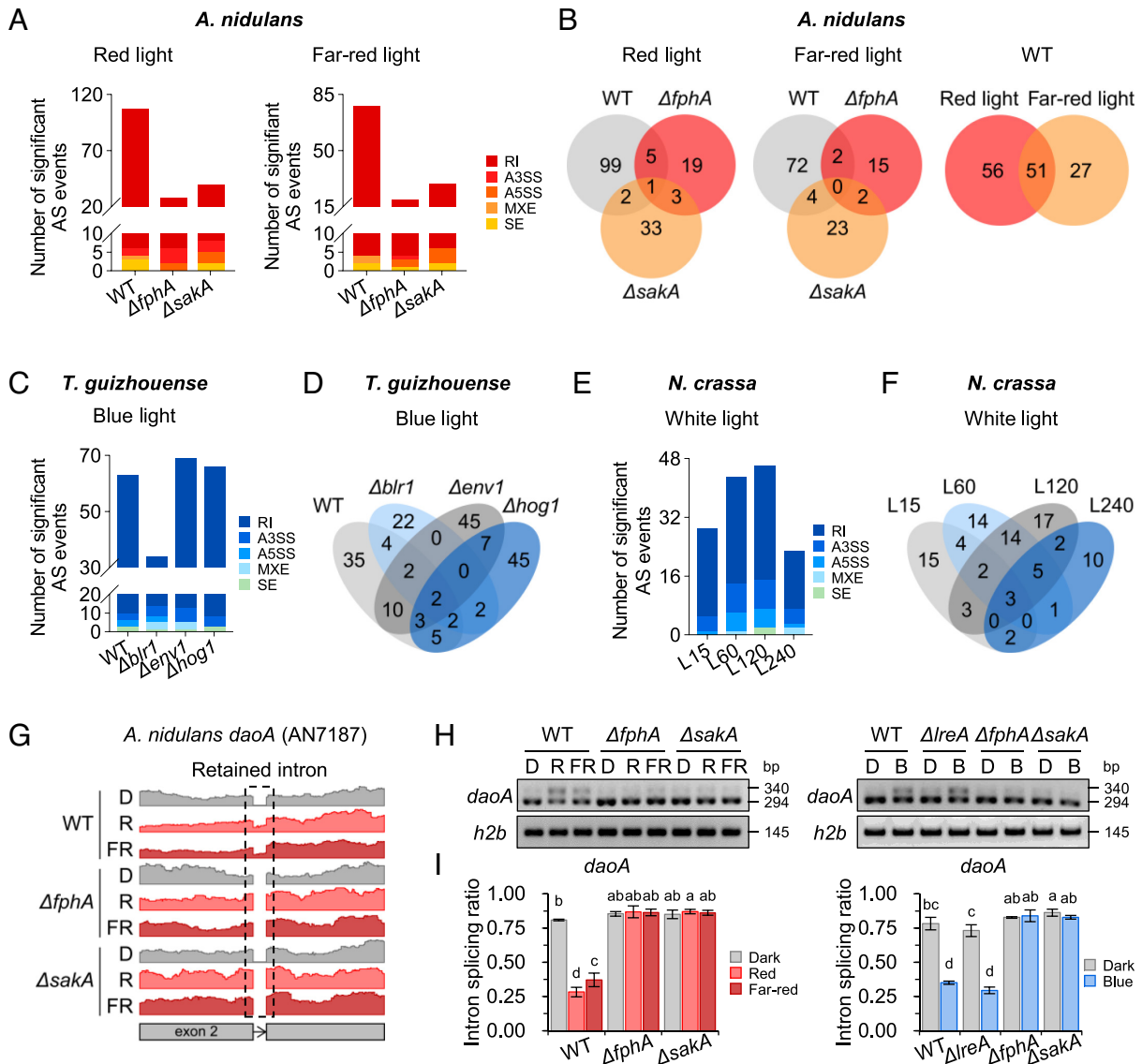


Fig. 1. Impact of light signals on AS in fungi. (A) Number of significant AS events in *A. nidulans* WT and its $\Delta fphA$ and $\Delta saka$ mutants after short-term red and far-red-light exposure. RI, retained intron; A3SS, alternative 3' splice site; A5SS, alternative 5' splice site; MXE, mutually exclusive exon; SE, skipped exon. (B) Venn diagrams of red and far-red-light-regulated AS events in different strains. (C) Number of significant AS events in *T. guizhouense* WT and its $\Delta blr1$, $\Delta env1$, and $\Delta hog1$ mutants after short-term blue light exposure. (D) The Venn diagram of blue light-regulated AS events in different strains. (E) Number of significant AS events in *N. crassa* after exposure to white light for 15 (L15), 60 (L60), 120 (L120), or 240 (L240) min. (F) The Venn diagram of white light-regulated AS events at four time points. (G) IGV analysis of red- and far-red-light-regulated AS of *daoA* (AN7187) in *A. nidulans* WT and its $\Delta fphA$ and $\Delta saka$ mutants. D, Dark; R, Red light; FR, Far-red light. (H) sqPCR analysis of red-, far-red-, and blue-light-regulated AS of *daoA* in *A. nidulans* WT and its $\Delta lreA$, $\Delta fphA$, and $\Delta saka$ mutants. The *h2b* gene was used for normalization. D, Dark; R, Red light; FR, Far-red light; B, Blue light. (I) Intron splicing ratios of *daoA* in different strains upon different wavelengths of light exposure. Statistical analysis was performed using one-way ANOVA followed by Tukey's test, and different lowercase letters represent significant difference ($P < 0.05$). Comparisons were made among all groups shown in each figure.

RI of *daoA* (AN7187), which encodes an amino acid oxidase in *A. nidulans*, was strictly dependent on FphA and Saka (Fig. 1 G–I). Interestingly, we found that blue light can also induce RI of *daoA*, while this process depended on FphA and Saka rather than the blue light receptor LreA (Fig. 1 H and I), which was consistent with the previous study that FphA and Saka participate in blue light sensing in *A. nidulans* (22). Similarly, the *naxe* (OPB45269), which encodes an NAD(P)H-hydrate epimerase in *T. guizhouense*, also showed BLR1- and HOG1-dependent AS pattern under blue light (SI Appendix, Fig. S2). Together, these data further confirm the importance of photoreceptors and the MAPK HOG (Sak) pathway for light-regulated AS.

Light-Regulated AS Is Involved in Several Biological Processes.

Long-term blue light exposure regulates diverse biological processes in *T. guizhouense*, such as conidiation and stress

resistance (19). To investigate its impact on AS, we performed the transcriptome analysis of *T. guizhouense* after constant blue light exposure. In WT, 122 blue light-regulated AS events of 117 genes were detected, nearly double the number identified after short-term blue light exposure (SI Appendix, Fig. S3 A and B and Dataset S1F). Among these, 48 events exhibited enhanced splicing patterns, while 74 events showed repressed splicing patterns. Notably, these events were predominantly regulated by the blue light receptor BLR1 and MAPK HOG1, similar to those regulated by short-term exposure (SI Appendix, Fig. S3B). In addition, AS of nine genes was coregulated by short-term and constant blue light exposure (SI Appendix, Fig. S3C). These findings reveal the dynamic regulation of AS by light and highlight the critical roles of BLR1 and HOG1 in blue light-regulated AS.

To gain insights into the functions of light-regulated AS, we performed KEGG pathway enrichment analysis on genes with

light-regulated AS events. Three fungi exhibited similar enriched pathways, such as signal transduction, cell cycle control, and secondary metabolism (SI Appendix, Fig. S4). These findings suggest that light-regulated AS probably participates in diverse key processes.

Blue Light-Regulated AS and Gene Transcription Are Both Involved in Blue Light-Repressed Ergothioneine Production in *T. guizhouense*. Through transcriptome analysis, we found that both introns of OPB36482 were retained under blue light in *T. guizhouense* WT and the blue light receptor mutant $\Delta env1$, with the retention of the first intron (Intron 1) leading to premature translation termination (Fig. 2 A–C and SI Appendix, Fig. S5 A and B). In *T. guizhouense*, this splicing pattern was abolished in

the blue light receptor mutant $\Delta blr1$, indicating that it is BLR1-dependent (Fig. 2 A and B and SI Appendix, Fig. S5A). However, in the MAPK HOG1 mutant, the splicing pattern was just slightly altered, suggesting that HOG1 is not as important as BLR1 in this case.

Functional characterization via BLASTP identified the OPB36482-encoded protein as a putative ortholog of *N. crassa* EGT1, an enzyme involved in ergothioneine biosynthesis (sequence identity: 35.9%, e-value: 6.7e-15). Ergothioneine is an efficient antioxidant produced by many organisms (23). In *N. crassa*, two enzymes EGT1 and EGT2 are required to convert histidine, S-adenosylmethionine, and cysteine into ergothioneine (Fig. 2D) (24). In *T. guizhouense*, two putative orthologs of *N. crassa* EGT1 were identified: OPB45450 (EGT1a, sequence

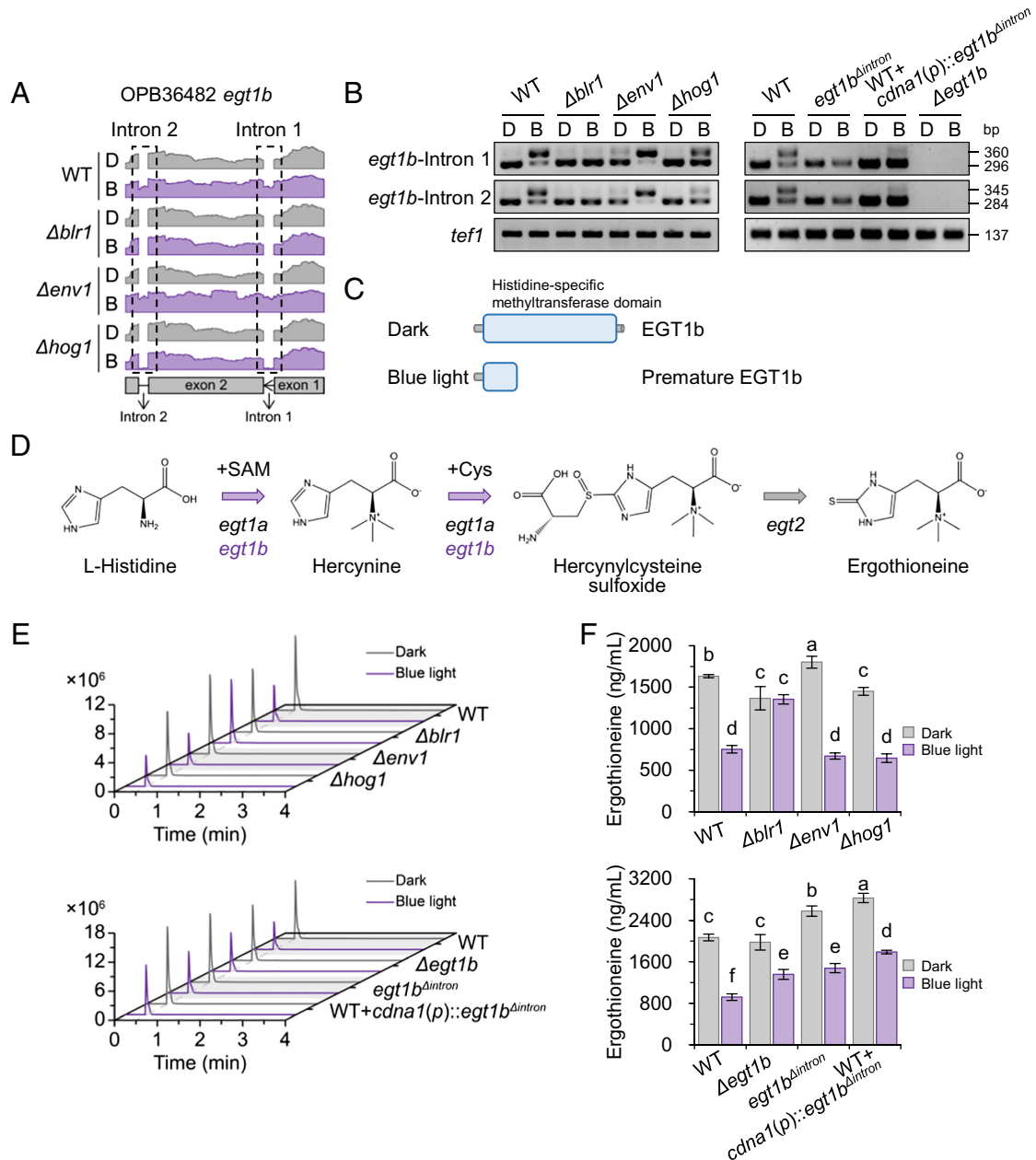


Fig. 2. Blue light-induced AS regulates ergothioneine (EGT) production in *T. guizhouense*. (A) IGV analysis of blue light-regulated retention of Intron 1 and 2 of *egt1b* (OPB36482) in WT and its $\Delta blr1$, $\Delta env1$, and $\Delta hog1$ mutants. D, Dark; B, Blue light. (B) sqPCR analysis of blue light-regulated retention of Intron 1 and 2 of *egt1b* in WT and its $\Delta blr1$, $\Delta env1$, $\Delta hog1$, *egt1b^{Δintron}*, WT+*cdna1(p)::egt1b^{Δintron}*, and $\Delta egt1b$ mutants. The expression level of each gene was normalized to the *tef1* gene. (C) Predicted domain structure of EGT1b and truncated EGT1b due to intron retention under blue light. (D) The biosynthetic pathway of EGT in fungi. (E) Extracted ion chromatograms of EGT (*m/z* 229.3 [M + H]⁺) from LC-MS analysis of different strains. (F) EGT contents in different strains under dark and blue light conditions. Data represent mean ± SD (n = 3). Statistical analysis was performed using one-way ANOVA followed by Tukey's test, and different lowercase letters represent significant difference (*P* < 0.05). Comparisons were made among all groups shown in each figure.

identity: 62.1%; e-value: 0) and OPB36482 (EGT1b). EGT1b shares 35.2% identity with EGT1a (e-value 2.7e-16). The amino acid sequence of the truncated EGT1b is identical to the N-terminal sequence of the full-length EGT1b and shares 30.0% identity with EGT1a (e-value: 2.1e-07) in *T. guizhouense*. One putative ortholog of *N. crassa* EGT2 was identified: OPB40377 (EGT2, sequence identity: 61.2%; e-value: 27e-56). EGT1a consists of a histidine-specific methyltransferase domain, a DinB_2 superfamily domain and a sulfatase domain, EGT1b only contains a histidine-specific methyltransferase domain, and EGT2 contains an aminotransferase domain (SI Appendix, Fig. S5C). It is worth mentioning that among these genes related to ergothioneine biosynthesis in the three fungi analyzed in this work, only *egt1b* in *T. guizhouense* exhibited light-regulated AS.

To investigate whether blue light regulates ergothioneine production, we quantified ergothioneine contents in WT and the $\Delta blr1$, $\Delta env1$, and $\Delta hog1$ mutants using LC-MS/MS. In WT, blue light exposure resulted in a 53.9% reduction in ergothioneine content compared to darkness, and similar reductions were observed in $\Delta env1$ (62.7%) and $\Delta hog1$ (55.5%) mutants (Fig. 2 E and F), indicating HOG1 is not important for ergothioneine production although the absence of HOG1 slightly altered the splicing pattern of *egt1b*. In contrast, no significant change was detected in the $\Delta blr1$ mutant under blue light. These results suggest that blue light represses ergothioneine biosynthesis in a BLR1-dependent manner.

We measured transcript levels of *egt1a*, *egt1b*, and *egt2* and found that blue light significantly repressed the transcription of *egt1b* through BLR1, whereas the transcription of *egt1a* or *egt2* was not affected (SI Appendix, Fig. S5D). In addition, transcriptome analysis showed that neither transcripts of *egt1a* nor *egt2* exhibited light-regulated AS. The results indicate the role of BLR1-mediated transcriptional regulation of *egt1b* in blue light-repressed ergothioneine production.

To further analyze whether the retention contributes to this process, we constructed an *egt1b* intron-deletion mutant (*egt1b* ^{Δ intron}) lacking both introns (Intron 1 and 2), an *egt1b* overexpression mutant (WT+*cdna1*(p)::*egt1b* ^{Δ intron}) constructed by transforming a plasmid harboring the *T. reesei* *cdna1* promoter-driven *egt1b* gene lacking both introns into WT, and an *egt1b*-deletion mutant (Δ *egt1b*). sqPCR and intron splicing ratio analysis confirmed that both introns of *egt1b* were completely removed in the *egt1b* ^{Δ intron} mutant (Fig. 2B and SI Appendix, Fig. S5A). After blue light exposure, the proportion of spliced transcripts in the overexpression mutant (WT+*cdna1*(p)::*egt1b* ^{Δ intron}) was significantly higher than that in WT and it is worth noting that the upper bands indicating the retention of Intron 1 and 2 resulted from the endogenous WT *egt1b* (Fig. 2B and SI Appendix, Fig. S5A). PCR analysis confirmed that the overexpression construct was randomly integrated into the genome and that the endogenous *egt1b* locus remained intact (SI Appendix, Fig. S5 E–G).

Compared to WT, the ergothioneine content in the *egt1b* ^{Δ intron} mutant increased by 24.6% in the dark and 61.0% in blue light (Fig. 2 E and F), suggesting that the negative role of intron retention in ergothioneine production. The *egt1b* overexpression mutant (WT+*cdna1*(p)::*egt1b* ^{Δ intron}) exhibited even greater increases (36.8% in the dark and 94.6% in blue light), suggesting the contribution of *egt1b* to ergothioneine production. However, the ergothioneine content in the Δ *egt1b* mutant was comparable to WT in the dark, and moreover, the content in the Δ *egt1b* was significantly higher than that in WT under blue light. We then measured transcript levels of *egt1a* and *egt2* in the Δ *egt1b* mutant and found that the transcription of *egt1a* and *egt2* was decreased

in the absence of EGT1b after blue light exposure (SI Appendix, Fig. S5D). These results suggest the unknown compensatory mechanism for the regulation of ergothioneine biosynthesis, which probably is activated when EGT1b is absent and not repressed by light. Together, these results indicate that blue light can repress ergothioneine biosynthesis, with BLR1-dependent transcription and AS of *egt1b* both involved in this process.

CRG1 Represses Conidiation, and Light-Enhanced Intron Retention Attenuates Its Repressive Function in *T. guizhouense*.

Among the nine genes whose AS is coregulated by short-term and constant blue light exposure, OPB44844, encoding a Zn₂Cys₆-type transcription factor, showed blue light-enhanced retention of the second intron in WT and the blue light receptor mutant $\Delta env1$ (SI Appendix, Figs. S6 A and B and S7 A and B). It is worth noting that its orthologs in *A. nidulans* (AN4197) and *N. crassa* (NCU07745) did not exhibit light-regulated AS, suggesting that this splicing response is species-specific. In *T. guizhouense*, this retained intron results in an additional 40 amino acid sequence, which is located adjacent to the DNA-binding domain and does not disrupt the key functional domains of the protein (SI Appendix, Figs. S6C and S7A). No splicing changes were found in the blue light receptor mutant $\Delta blr1$ and the MAPK HOG1 mutant $\Delta hog1$ under dark and blue light conditions, indicating that its AS is regulated by BLR1 and HOG1 (SI Appendix, Figs. S6 A and B and S7B).

Blue light-induced conidiation is a hallmark of *T. guizhouense* photobiology, and it is abolished in the absence of the blue light receptor BLR1 and markedly repressed in the absence of the MAPK HOG1 (25). We found that, compared to WT, the absence of OPB44844 increased conidia production by 41.7% and 9.3% after 2 and 3 d of culture, respectively (SI Appendix, Fig. S6 D and E). We further measured OPB44844 transcript levels and found that blue light can induce its transcription through BLR1 (SI Appendix, Fig. S7C). Transcriptome analysis showed that the transcription of its orthologs in *A. nidulans* and *N. crassa* was not activated by light. These findings suggest that OPB44844 is transcriptionally activated by blue light and functions to repress conidiation in *T. guizhouense*. Therefore, we named OPB44844 as *crg1* (conidiation repressor gene 1).

To further explore whether the light-regulated AS of *crg1* contributes to its repressive function, we constructed a *crg1* deletion mutant (Δ *crg1*), a *crg1* intron-deletion mutant (*crg1* ^{Δ intron}) lacking all introns, and a *crg1* overexpression mutant (WT+*tef1*(p)::*crg1* ^{Δ intron}), constructed by transforming a plasmid harboring the *T. reesei* *tef1* promoter-driven *crg1* gene without introns into WT. sqPCR and intron splicing ratio analysis confirmed that the second intron of *crg1* was completely removed in the *crg1* ^{Δ intron} mutant (SI Appendix, Figs. S6B and S7B). The proportion of spliced transcripts in the WT+*tef1*(p)::*crg1* ^{Δ intron} mutant was significantly higher than that in WT after blue light exposure, and the upper bands indicating the retention of the second intron resulted from the endogenous WT *crg1* (SI Appendix, Figs. S6B and S7B). PCR analysis confirmed that the overexpression construct was randomly integrated into the genome and that the endogenous *crg1* locus remained intact (SI Appendix, Fig. S7 D–F).

Compared to WT, the *crg1* ^{Δ intron} mutant exhibited reduced conidia production by 18.0% and 1.6% after 2 and 3 d of culture, respectively, suggesting that removal of the second intron enhances the conidiation repression activity of *crg1* (SI Appendix, Fig. S6 D and E). Among all mutants, the *crg1* overexpression mutant (WT+*tef1*(p)::*crg1* ^{Δ intron}) produced the fewest conidia, with reductions of 34.7% and 22.7% compared to WT after 2 and 3 d, respectively, suggesting that the conidiation repression ability of

crg1 was further enhanced. These data indicate that light-enhanced intron retention attenuates the repressive function of CRG1 in conidiation.

Collectively, *crg1* is transcriptionally activated by blue light to repress conidiation in *T. guizhouense*, while blue light-regulated intron retention of its transcripts can attenuate this repressive function, which is regulated by photoreceptors and the MAPK HOG1.

The Serine/Threonine Kinase SRK1 Is Involved in Blue Light Signal Transduction from HOG1 to Modulate AS Efficiency. To explore how the MAPK HOG pathway regulates AS in *T. guizhouense*, we analyzed transcriptome data and identified *srk1*, the ortholog of *A. nidulans srkA*, which was significantly upregulated by the blue light receptor BLR1 and MAPK HOG1 under blue light. In *A. nidulans*, SrkA functions downstream of the MAPK SakA to regulate oxidative stress responses and development (26). We measured *srk1* transcript levels and found that its expression was significantly increased after 45 min of blue light exposure in WT and the blue light receptor $\Delta env1$ but remained unchanged in $\Delta blr1$ and $\Delta hog1$ mutants (Fig. 3A). In addition, the basal transcript level of *srk1* in the dark was significantly reduced in the absence of HOG1 compared to that in WT and the $\Delta blr1$ mutant. We also performed western blot analysis of GFP-tagged SRK1 and found that SRK1 protein levels increased significantly after 10 min of blue light exposure in WT (Fig. 3B). In the $\Delta blr1$ mutant, SRK1 protein levels remained unchanged under dark and blue light conditions. Notably, the protein level of SRK1 in the $\Delta hog1$ mutant was significantly lower than those in WT and the $\Delta blr1$ mutant under both conditions. These data demonstrate that BLR1 and HOG1 control the blue light-induced SRK1 expression, and moreover, HOG1 maintains the basal expression of SRK1 in the dark, potentially through regulation of mRNA translation efficiency or protein stability with an unknown HOG1-dependent mechanism. To evaluate the role of SRK1 in blue light-regulated AS in *T. guizhouense*, we constructed the $\Delta srk1$ mutant and analyzed splicing patterns of three selected genes

exhibiting light-regulated AS in the transcriptomes of WT: *crg1* (AS regulated by both short-term and constant blue light), *naxe* (AS regulated only by short-term blue light), and *fgl1* (encoding a globin-like protein, and AS regulated only by constant blue light). For *crg1*, the splicing ratio was reduced when SRK1 was absent, with no significant difference under short-term blue light exposure, but decreased significantly under constant blue light exposure (Fig. 3C and D). The intron splicing ratio of *naxe* was also reduced in the $\Delta srk1$ mutant, and AS of *fgl1* was not regulated by blue light anymore. Thus, these results reveal that blue light can induce SRK1 expression through the MAPK HOG pathway to regulate AS efficiency in *T. guizhouense*.

SRK1 Interacts with SRP1 in the Nucleus and Regulates Vegetative Growth and Conidiation in Blue Light. To identify SRK1 targets involved in AS regulation, we performed IP-MS using an SRK1-GFP tagged strain under dark and blue light conditions, with a GFP-expressing strain in the WT background as a control (SI Appendix, Fig. S8). 26 and 9 putative interacting proteins were identified in the dark and blue light, respectively (SI Appendix, Table. S1). Notably, MAPK HOG1 was identified in the dark, and the serine/arginine-rich (SR) protein SRP1, a splicing factor crucial for spliceosome assembly and exon recognition (27), was specifically identified after 10 min of blue light exposure. Co-IP confirmed robust interactions between SRK1 and HOG1 under both dark and blue light conditions and between SRK1 and SRP1 only in blue light (Fig. 4A).

To further investigate the roles of SRK1 and SRP1 in blue light responses, we constructed gene deletion ($\Delta srk1$ and $\Delta srp1$) and complemented (*srk1^c* and *srp1^c*) mutants and verified these mutants by diagnostic PCR and Southern blot analysis (SI Appendix, Fig. S9). The absence of SRK1 and SRP1 showed similar phenotypes, with conidiation and vegetative growth strongly inhibited in blue light (Fig. 4B–D). While the vegetative growth was also inhibited in the dark, it was more sensitive to blue light. In the $\Delta srk1$ mutant, conidia production was decreased by 83.5% after 3 d in blue light, and the colony diameter was reduced

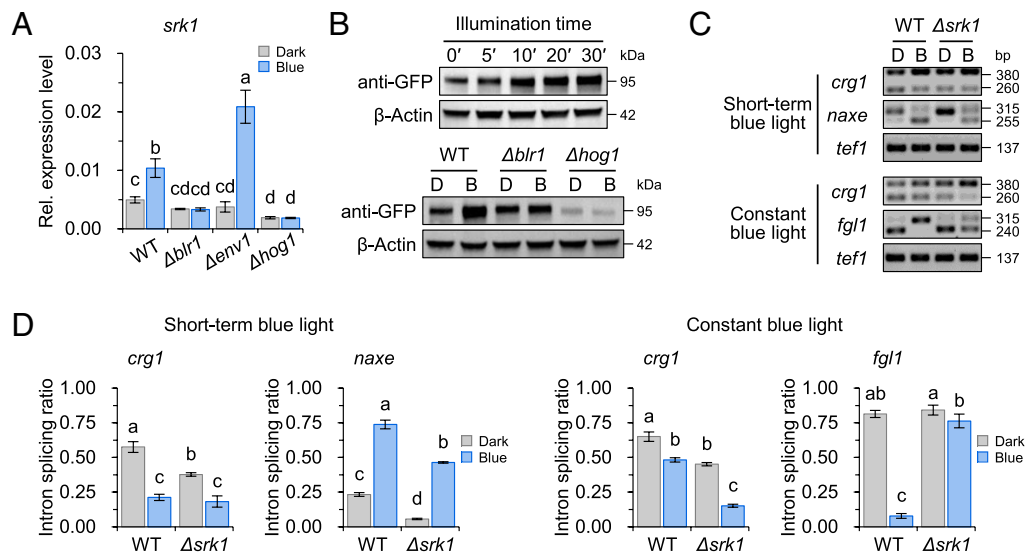


Fig. 3. Blue light activates SRK1 through the MAPK HOG pathway to affect AS efficiency in *T. guizhouense*. (A) Transcript levels of *srk1* in different strains under dark and blue light conditions. WT and its $\Delta blr1$, $\Delta env1$, and $\Delta hog1$ mutants were cultured in the dark for 24 h and then exposed to blue light for 45 min. (B) Protein expression of SRK1 under different blue light exposure times (Left) and in different strains (Right). Left: WT was grown in the dark for 24 h before exposure to blue light for 5, 10, 20, and 30 min. Right: WT and its $\Delta blr1$, $\Delta env1$, and $\Delta hog1$ mutants were cultured in the dark for 24 h and then exposed to blue light for 10 min. β -Actin was used for normalization. (C) sqPCR analysis of blue light-regulated AS in WT and the $\Delta srk1$ mutant. (D) Intron splicing ratios of each gene in WT and the $\Delta srk1$ mutant upon different times of blue light exposure. The expression level of each gene was normalized to the *tef1* gene. Error bars represent the SD of three biological replicates. Statistical analysis was performed using one-way ANOVA followed by Tukey's test, and different lowercase letters represent significant difference ($P < 0.05$). Comparisons were made among all groups shown in each figure.

by 55.5% after 2 d in blue light (Fig. 4 C and D). Similarly, in the $\Delta srp1$ mutant, conidia production was decreased by 89.1%, and the colony diameter was reduced by 56.9% under the same conditions. Complementation of SRK1 or SRP1 recovered both conidiation and vegetative growth to WT levels. These results indicate that SRK1 and SRP1 regulate vegetative growth and conidiation in *T. guizhouense* under blue light.

Previous studies have shown that MAPK SakA (HOG1) can shuttle into the nucleus in response to light and various stresses in fungi (18, 19, 28, 29). The physical interaction between HOG1 and SRK1 and blue light-triggered interaction between SRK1 and SRP1 prompted us to further investigate the subcellular localization of SRK1 and SRP1 under different conditions. Fluorescence microscopy showed that SRP1-GFP signals were stably concentrated in the nucleus under dark, blue light, and oxidative stress conditions, indicating SRP1 as a nuclear protein (Fig. 4E). For SRK1, GFP signals were evenly distributed in the cytoplasm in the dark but translocated to the nucleus within 5 min of blue light or oxidative stress exposure (Fig. 4F). In summary, these findings demonstrate that SRK1 functions downstream of the MAPK-HOG pathway and interacts with SRP1 in the nucleus to further transmit the blue light signal in *T. guizhouense*.

Blue Light Regulates the Phosphorylation of SRK1 and SRP1 to Modulate Blue light-Regulated AS Efficiency in *T. guizhouense*.

To evaluate whether blue light regulates the phosphorylation levels of SRK1 and SRP1, we performed phos-tag assays using SRK1-GFP tagged strains in WT and the $\Delta bbl1$ and $\Delta hog1$ mutants and SRP1-GFP tagged strains in WT and the $\Delta bbl1$, $\Delta hog1$, and $\Delta srk1$ mutants. After 10 min of blue light exposure, more phosphorylated SRK1 (SRK1-p) was present in WT, whereas no changes were observed in the $\Delta bbl1$ mutant (Fig. 4G). Remarkably, the SRK1 protein was hardly detectable in the $\Delta hog1$ mutant and the signal of phosphorylated SRK1 was very weak. LC-MS/MS identified 314 T as the putative phosphorylation site of SRK1 and confirmed that its phosphorylation level was elevated in WT upon blue light exposure (Fig. 4H). Conversely, phosphorylated SRP1 (SRP1-p) levels were decreased in WT and the $\Delta bbl1$ mutant under blue light and further reduced in the absence of HOG1 or SRK1 (Fig. 4G). However, the unphosphorylated SRP1 levels were not increased in $\Delta bbl1$ and $\Delta srk1$ and they were even decreased after blue light exposure in WT, suggesting that blue light regulate the protein abundance of SRP1. LC-MS/MS identified 111S and 113S as putative phosphorylation sites of SRP1 and validated the decreased phosphorylation level of SRP1 in WT after blue light exposure (Fig. 4H). These data suggest that blue light could modulate both protein abundance and phosphorylation of SRK1 and SRP1 in *T. guizhouense*.

We then analyzed the transcriptomes of $\Delta srk1$ and $\Delta srp1$ mutants of *T. guizhouense* after short-term and constant blue light exposure. After short-term blue light exposure, 77.1% (37/48) blue light-regulated AS events were regulated by SRK1, 72.9% (35/48) events were regulated by SRP1, and 64.6% (31/48) events were coregulated by SRK1 and SRP1 (Fig. 4 I and J). 85.7% (66/77) events in the $\Delta srk1$ mutant, and 81.2% (56/69) events in the $\Delta srp1$ mutant were not detected in WT. Among 37 SRK1- and 35 SRP1-regulated events, RI, A3SS, and A5SS were the predominant types (SI Appendix, Fig. S10A). Similarly, after constant blue light exposure, 70.5% (86/122) blue light-regulated AS events were regulated by SRK1, 69.7% (85/122) events were regulated by SRP1, and 56.6% (69/122) events were coregulated by SRK1 and SRP1 (Fig. 4 I and J). 64.7% (66/102) events in the $\Delta srk1$ mutant, and 67.5% (77/114) events in the $\Delta srp1$ mutant were not detected in WT (Fig. 4J). RI was the most frequent type

among 86 SRK1- and 85 SRP1-regulated events (SI Appendix, Fig. S10A). Analysis of previously selected genes also showed that the absence of SRP1 results in a similar splicing pattern to that detected in the $\Delta srk1$ mutant (SI Appendix, Fig. S10 B and C). Additionally, compared to WT in the dark, 81 and 211 AS events were also identified in $\Delta srk1$ and $\Delta srp1$ mutants, respectively, with 39 events shared between them (SI Appendix, Fig. S11). Collectively, these data suggest that blue light could regulate AS efficiency by modulating SRK1 and SRP1 phosphorylation, and SRK1 and SRP1 are also important for maintaining basal splicing regulation in the dark in *T. guizhouense*.

Discussion

AS is an important regulatory strategy for fungal adaptation to environmental changes. In *N. crassa*, temperature-dependent splicing of the circadian clock gene *frq* fine-tunes the circadian rhythm in response to ambient temperature (30). In the human pathogen *Pneumocystis carinii*, host-associated conditions induce AS of the inosine monophosphate dehydrogenase (IMPDH) gene to support survival and virulence, while in *Trichophyton rubrum*, undecanoic acid-induced AS of IMPDH gene facilitates its adaptation to fatty acid toxicity (31, 32). This study shows that AS is important for some fungal light responses. Transcriptome analysis of *A. nidulans*, *T. guizhouense*, and *N. crassa* demonstrates that light regulates AS in addition to gene transcription, adding a level of complexity for light signaling in fungi. Instead of focusing mainly on transcriptional gene activation, future studies on fungal environmental responses should also pay attention to AS.

Notably, light-regulated AS in *N. crassa* displayed dynamic changes across different durations of light exposure, and prolonged blue light exposure was accompanied by an increase in AS events in *T. guizhouense*. Since constant light exposure accelerates the transition from vegetative growth to conidiation in fungi (17, 19, 33), this suggests the dynamic regulation of AS by light and its potential associations with distinct fungal developmental stages. Such stage-specific AS has been reported in *N. crassa*, where intron retention of *cox-5* (encoding cytochrome c oxidase subunit V) was detected in dormant conidia but not in germinating spores or hyphae (34). Interestingly, retained introns were the most frequent AS pattern in three fungi, with light signals exhibiting dual roles in either promoting or suppressing intron splicing. This raises the intriguing possibility that light signals are dispersed to both splicing enhancers and suppressors, but the detailed mechanisms remain to be elucidated.

Light has been shown to regulate AS in plants, with well-characterized regulatory mechanisms (35). Phytochrome-regulated AS modulates plant light responses, such as photomorphogenesis and hypocotyl elongation (20). Beyond the phytochrome-dependent signaling pathway, light modulates AS in plants through multiple mechanisms, such as chloroplast retrograde signaling, the splicing regulator PICLN, the TOR kinase pathway, and the regulation of transcriptional elongation (36–39). These findings highlight the complexity of light-regulated AS in higher eukaryotes. Here, we provide an example showing how an environmental signal reaches the splicing machinery through a sensor protein and the downstream signaling pathway to regulate AS in fungi (Fig. 5). We reveal that in *A. nidulans* and *T. guizhouense* the light-regulated AS is controlled by photoreceptors and the MAPK HOG (Sak) pathway, with the serine/threonine kinase SRK1 as a key downstream target of HOG1 in *T. guizhouense*. HOG1 and SRK1 orthologs in other fungi have been reported to mediate responses to oxidative and osmotic stresses (26, 40, 41), suggesting the potential roles of AS in the responses of other environmental

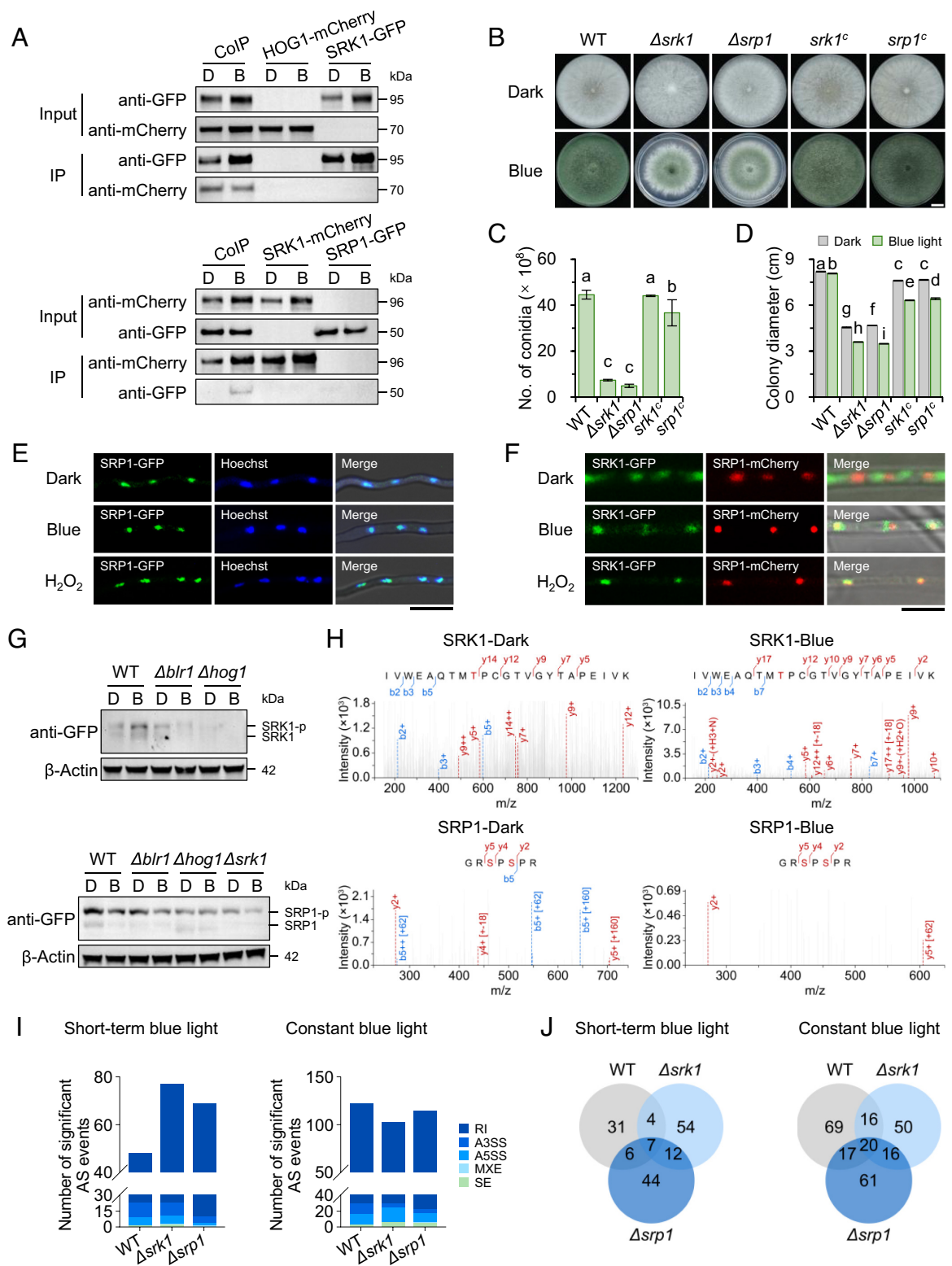


Fig. 4. Blue light induces SRK1 to interact with SRP1 in the nucleus through the MAPK HOG pathway. (A) Coimmunoprecipitation (Co-IP) assays between HOG1-GFP and SRK1-mCherry, and between SRK1-mCherry and SRP1-GFP. Total and eluted proteins were detected by western blot using anti-GFP or anti-mCherry antibodies. (B) Phenotype analysis of WT and its $\Delta srk1$, $\Delta srp1$, $srk1^c$, and $srp1^c$ mutants after grown in dark and blue light for 3 d. (Scale bar, 1 cm.) (C) Quantification of conidia produced by each strain after 3 d of blue light exposure. (D) Colony diameters of each strain under blue light and dark conditions after 2 d of culture. Statistical analysis was performed using one-way ANOVA followed by Tukey's test, and different lowercase letters represent significant difference ($P < 0.05$). Comparisons were made among all groups shown in each figure. Error bars represent the SD of three biological replicates. (E) Subcellular localization of SRP1 under dark, blue light, and oxidative stress conditions. The SRP1-GFP tagged strain was incubated on microscope coverslips with 400 μ L PDB in the dark for 14 h and then exposed to blue light or oxidative stress for 3 min. Samples were fixed with 4% formaldehyde in the dark for 10 min and then stained with Hoechst. (Scale bar, 5 μ m.) (F) Subcellular localization of SRK1 upon the same conditions in SRK1-GFP and SRP1-mCherry double-tagged strains. (Scale bar, 3 μ m.) (G) Phosphorylation levels of SRK1 and SRP1 in WT and mutants under dark and blue light conditions were detected using phos-tag gels followed by western blot. β -Actin protein was used for normalization. (H) Phosphorylation sites of SRK1 and SRP1 identified by LC-MS/MS in WT. Red and blue text indicate the detected b and y ions, respectively, which confirm peptide sequence and phosphorylation site assignment. (I) Number of significant AS events in $\Delta srk1$ and $\Delta srp1$ mutants after short-term and constant blue light exposure. (J) Venn diagrams of significant AS events in different mutants.

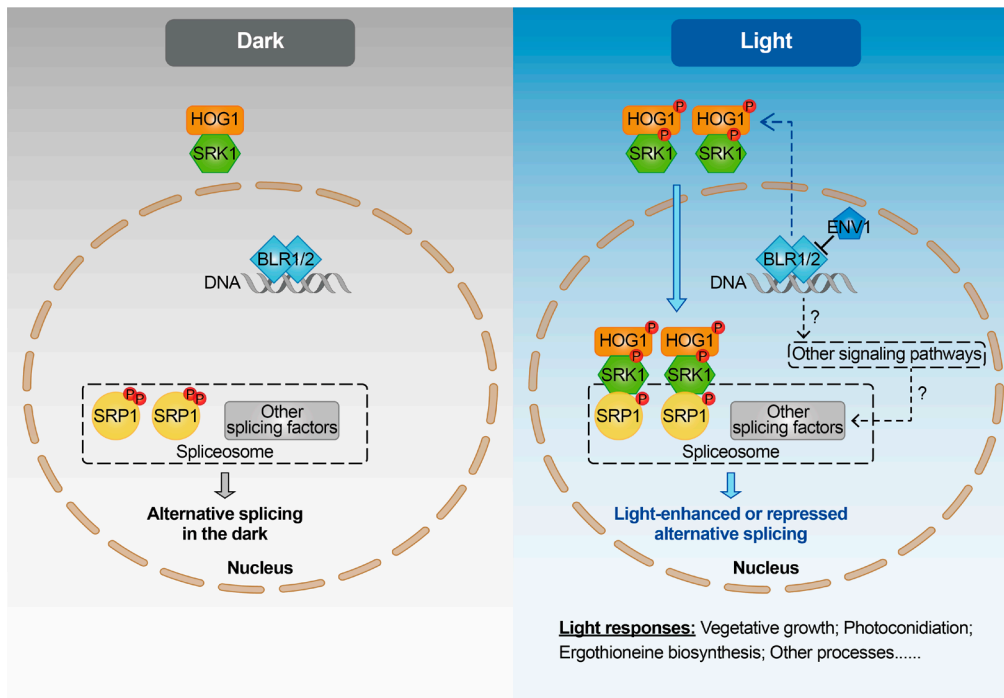


Fig. 5. Model of light-regulated AS in *T. guizhouense*.

signals. Notably, a number of light-regulated AS events were identified in the absence of photoreceptors and MAPK HOG1 (SakA), with only a few shared with those detected in WT. This finding suggests that light may also regulate fungal AS through other photoreceptors or unknown signaling pathways.

We further found that in *T. guizhouense* SRK1 transmits blue light signals from the cytoplasm to the nucleus, where it interacts with the nuclear-localized splicing factor SRP1 to coregulate AS efficiency. Posttranslational modifications (PTMs) of splicing factors are critical for regulating AS, such as ubiquitination of Sde2 in *Schizosaccharomyces pombe*, methylation of MoSNP1, and SUMOylation of MoSrp1 in *Magnaporthe oryzae* (27, 42, 43). In addition, protein arginine methyltransferase 5 (PRMT5)-mediated arginine methylation has been shown to regulate AS of thaumatin-like protein pre-mRNA in the medicinal mushroom *Ganoderma lucidum*, thereby affecting downstream metabolic processes such as polysaccharide biosynthesis (44). Here, increased SRK1 phosphorylation and decreased SRP1 phosphorylation in *T. guizhouense* under blue light suggest distinct roles in AS regulation. Increased SRK1 phosphorylation likely activates its function in signal transduction, while reduced SRP1 phosphorylation may stabilize its nuclear localization or facilitate its interactions with spliceosomal components, thus promoting precise splicing site selection or efficient spliceosome assembly.

Fungal AS regulates enzyme and secondary metabolite production. In the industrial fungi, substrate-dependent AS of exocellobi-ohydrolase I-like genes in *Phanerochaete chrysosporium* and the endoglucanase gene in *Mucor circinelloides* modulates cellulose degradation efficiency, enabling adaptive enzyme function in response to different carbon sources (45, 46). In the mushroom *Terana caerulea*, light mediates AS of *corA*, a gene encoding a poly-poric acid synthetase involved in corticin pigment biosynthesis (47). An interesting finding in this study is that blue light represses ergothioneine production in *T. guizhouense* by inducing intron retention of *egt1b*, with the retained intron directly disrupting translation. Although blue light also downregulates *egt1b* transcription, intron retention exerts a more direct impact on translation by

generating nonfunctional transcripts. This reveals the function of AS in the regulation of secondary metabolism during light responses and suggests that *T. guizhouense* likely preserves histidine, the precursor for ergothioneine biosynthesis, to balance energy and metabolic demands under environmental changes. Interestingly, *egt1b* is present in *T. guizhouense* but absent in *N. crassa*, and even in its absence, the strain still produced a certain amount of ergothioneine, suggesting the existence of compensatory mechanisms in its biosynthetic pathway. The nutraceutical value of ergothioneine is well known, with fungi as its primary natural source (23). Recent advances in its biosynthesis through metabolic engineering have been widely reported (48, 49). Our study suggests that manipulating AS could be a unique approach to enhance the biosynthesis of high-value nature products in the future.

In this work, a negative conidiation regulator encoding gene *crg1* was identified in *T. guizhouense*. Light induced its transcription, and moreover, AS was shown to weaken its function. The retained intron, adjacent to the DNA-binding domain, may affect the stability or activity of the protein to mediate protein–DNA interactions. This finding expands our understanding that AS, in addition to gene transcription, also contributes to light-regulated conidiation in fungi. Conidial transcription can be modulated according to environmental conditions and further affect the fitness and germination potential (50). Based on this, it is possible that AS plays a role in generating transcriptional variation, thereby facilitating conidia dispersal and survival under diverse environments.

Materials and Methods

Strains and Culture Conditions. The WT strains used in this study were *A. nidulans* FGSC A4 (*A. nidulans*) and *T. guizhouense* NJAU 4742 (*T. guizhouense*). *Escherichia coli* DH5 α (*E. coli*) was used for plasmid propagation and maintenance. *A. nidulans* was cultured on supplemented minimal medium at 37 °C (51), *T. guizhouense* was cultured on potato dextrose agar/broth (PDA/PDB) medium (BD Difco) at 28 °C, and *E. coli* was cultured on Luria-Bertani (LB) medium (Sangon Biotech) supplemented with 100 μ g/mL ampicillin at 37 °C. The intensity of specific wavelength of light used in this study was set to 1.7 μ mol photons/(m² × s)

by the self-made software designed previously (22). All strains used in this study are listed in *SI Appendix, Table. S2*.

Construction of Genetically Modified Strains. The $\Delta fphA$, $\Delta IreA$, and $\Delta saka$ mutants of *A. nidulans*, as well as the $\Delta blr1$, $\Delta env1$, and $\Delta hog1$ mutants of *T. guizhouense* were generated in previous studies (18, 19). Gene or intron deletion, gene complementation, and transformation of *T. guizhouense* were performed following a previously described procedure, and positive transformants were verified by PCR and Southern blot (52, 53). To construct the mutant with an overexpression allele of the target gene lacking introns, a plasmid containing the *hph* gene, along with the cDNA sequence of target gene under the control of the *T. reesei cdna1* or *tef1* promoter (54) was transformed into WT. To tag the target protein with a green/red fluorescent protein (GFP/mCherry), the fusion construct composed of the open reading frame of the target gene, *gfp/mcherry* with a synthetic linker (3 × GGGGS), a resistance cassette, and ~1.5 kb downstream flanking sequence of the target gene was generated and transformed into WT. *gfp* was fused to *hph* gene, and *mcherry* was fused to *neo1* gene. Positive transformants were verified by PCR. Primers used in this study are listed in *SI Appendix, Table. S3*.

RNA Extraction, qPCR, and Transcriptome Sequencing. To evaluate red- and far-red-light responses in *A. nidulans*, fresh conidia of WT and the $\Delta fphA$ and $\Delta saka$ mutants were inoculated on the surface of 4 mL liquid minimal medium (\emptyset 3 cm) containing 2% glucose, 1 μ g/mL pyridoxine HCl, 1 mg/mL uracil, and 1 mg/mL uridine and were cultured in the dark for 24 h. Afterward, red or far-red light was imposed for 20 min. To evaluate blue light responses in *T. guizhouense*, fresh mycelia of WT and the $\Delta blr1$, $\Delta env1$, and $\Delta hog1$ mutants were grown on 8 mL PDA medium (\emptyset 6 cm) covered with cellophane. For short-term blue light exposure, each strain was exposed to blue light for 45 min after 24 h of culture in the dark. For constant blue light exposure, each strain was cultured under dark or blue light conditions for 48 h. Mycelia were harvested in dim-green light and frozen in liquid nitrogen immediately. Three biological replicates were prepared for each condition. Total RNA extraction, cDNA synthesis, and qPCR assay were performed as previously described (25). The *h2b* gene (AN3469) of *A. nidulans* and the *tef1* gene (OPB38715) of *T. guizhouense* were used for normalization. The light-responsive transcriptome data of *N. crassa* were obtained from publicly available datasets (Accession No: PRJNA232306), as published by Wu et al. (21). Transcriptome sequencing was performed at Gene Denovo Biotechnology Co., Ltd following a previously described procedure (53).

AS Analysis. AS events were identified from the transcriptome data using rMATS (<http://mats-seq.sourceforge.net/index.html>). To identify light-regulated AS, significant AS events (FDR < 0.05) were identified based on the ratios of splice junction usage under specific light conditions compared to the ratios in the dark. The ratios of splice junction usage of different mutants were also compared to those of WT in the dark to analyze the involvement of photoreceptors, MAPK HOG1 (SakA), SRK1, and SRP1 in the regulation of AS. Significant AS events were categorized into skipped exon (SE), mutually exclusive exon (MXE), alternative 5' splice site (A5SS), alternative 3' splice site (A3SS), and retained intron (RI). To review the mapping result and analyze the AS pattern, the sequencing data were visualized using the Integrative Genomics Viewer (IGV), enabling the comparison of read distribution based on the annotation result. Validation of AS events was performed by sqPCR and qPCR. sqPCR was conducted to confirm the splicing pattern. Primers for sqPCR were designed to target the two exons flanking the intron (*SI Appendix, Fig. S12A*). qPCR was carried out to measure the splicing ratio by calculating the ratio of spliced RNA to total RNA (spliced RNA and unspliced RNA), with minor modifications as previously described (11). Primers were designed based on the same protocol (*SI Appendix, Fig. S12B*). All relative primers are listed in *SI Appendix, Table. S3*.

Protein Extraction and Western Blot Analysis. Fresh conidia (1×10^5 conidia/mL) of each strain were cultured in 50 mL PDB medium at 170 rpm in the dark for 24 h, then exposed to blue light for 10 min. To evaluate the effect of illumination time on protein expression, blue light was imposed for 5, 10, 20, or 30 min. Mycelia were harvested in dim-green light and frozen in liquid nitrogen immediately. For total protein extraction, samples were ground in liquid nitrogen and resuspended in 1 mL extraction buffer (50 mM Tris-HCl, pH 8.0, 150 mM NaCl, and 0.5% Triton X-100) supplemented with protease inhibitor cocktail (Yeasen, 20124E503) and phosphatase inhibitor cocktail (Beyotime, P1081). After incubation on ice (20 min) and centrifugation (13,200 rpm, 4 °C, 20 min), the

supernatant was collected and the protein concentration was quantified using the Bradford protein assay.

The supernatant was mixed with SDS-PAGE loading buffer and heated at 98 °C for 10 min. After denaturing, equal amounts of protein from each sample were separated on a 12% SDS-polyacrylamide gel and transferred onto a PVDF membrane. The β -Actin protein was used for normalization. Immunoblotting was performed following the standard procedure with anti-GFP (Yeasen, 31002ES60), anti-mCherry (Cell Signaling Technology, 43590S), or anti- β -Actin antibodies (Abmart, T40104S) at a dilution of 1:1000. Horseradish peroxidase (HRP)-conjugated secondary antibodies (Beyotime, A0216&A0208, dilution 1:1000) and BeyoECL Moon chemiluminescent solutions (Beyotime, P0018FS) were used for detection.

Co-IP Assays. An SRK1-GFP tagged strain was generated, and the WT expressing GFP alone was used as a control. After total protein extraction, equal amounts of protein were incubated with GFP-Trap agarose beads (ChromoTek, gtmA) according to the protocol. The elution from GFP-Trap beads was separated by SDS-PAGE and stained with silver reagent to confirm SRK1-GFP expression. Liquid chromatography-tandem mass spectrometry (LC-MS/MS) analysis was performed at SpecAlly Life Technology Co., Ltd to identify SRK1 coimmunoprecipitated proteins.

Co-IP was performed using strains coexpressing HOG1-mCherry/SRK1-GFP or SRK1-mCherry/SRP1-GFP, with single-tag strains serving as controls. Total protein extraction was performed as described above. For HOG1-SRK1 and SRK1-SRP1 interaction assays, equal amounts of protein from each sample were incubated with GFP-Trap or mCherry-Trap agarose beads (ChromoTek), respectively. Western blot analysis of total proteins and bead elution was performed with an anti-GFP antibody and an anti-mCherry antibody, respectively.

Phosphorylation Analysis. Total protein was extracted from WT and phosphorylation proteomics was performed at Shanghai Bioprofile Technology Co., Ltd to identify phosphorylation levels and sites of target proteins.

Phos-tag assays were performed to detect phosphorylation levels of SRK1 and SRP1. The SRK1-GFP fusion construct was introduced into WT and the $\Delta blr1$ and $\Delta hog1$ mutants. The SRP1-GFP fusion construct was introduced into WT and the $\Delta blr1$, $\Delta hog1$, and $\Delta srk1$ mutants. The total protein was separated on a 7.5% SDS-polyacrylamide gel containing 50 μ M Phos-tag and 100 μ M ZnCl₂ (FUJIFILM Wako, 198-17981) at 80 V and 4 °C for 3 h. Then, gels were equilibrated in transfer buffer with 10 mM EDTA for 20 min three times and followed by transfer buffer without EDTA for 10 min. Proteins were transferred to a PVDF membrane at 80 V and 4 °C for 16 h. Western blot analysis was then carried out using an anti-GFP antibody and an HRP-conjugated secondary antibody.

Fluorescence Microscopy. Fresh mycelia of each strain were grown on PDA medium in the dark for 24 h. For light stimuli, samples were exposed to blue light for 3 min. For oxidative stress, samples were treated with 1 × phosphate-buffered saline (PBS, pH 7.4) containing 10 mM hydrogen peroxide for 3 min. Samples were then fixed immediately in 1 × PBS containing 4% formaldehyde for 10 min and washed once with 1 × PBS. Nuclei were stained with Hoechst (Solarbio, C0031). Fluorescence was observed using a Microscope DM2000 (Leica) and photographed with an MDX10 system (Mshot).

Phenotypic Analysis. For conidiation assays, fresh mycelia of *T. guizhouense* strains were inoculated on 8 mL PDA medium (\emptyset 6 cm) under dark or blue light conditions for 3 d. Conidia were collected with 20 mL distilled water and the suspension was filtered with Miracloth (Millipore, Merck KGaA). The conidia amount was quantified using a hemocytometer. To assess colony growth, each strain was cultured on 20 mL PDA medium (\emptyset 9 cm) under dark and blue light conditions and the colony diameter was measured after 48 h of culture.

Ergothioneine Extraction and LC-MS/MS Analysis. Fresh mycelia of each strain were cultured on 8 mL cellophane-covered PDA medium (\emptyset 6 cm) in the dark and blue light for 3 d. Samples were then harvested and ground into fine powder using liquid nitrogen. For ergothioneine extraction, samples were thoroughly resuspended in 15 mL of 20% methanol with 0.1% formic acid followed by centrifugation at 13,200 rpm for 10 min. The supernatant was then filtered through a 0.22 μ m organic-system filter for LC-MS/MS analysis.

Chromatographic separation was performed on a Kinetex F5 column (100 Å, 2.6 μ m, 100 × 2.1 mm; Phenomenex) at 40 °C with a flow rate of 0.4 mL/min using a

Triple Quad 6500+ system (AB SCIEX). The injection volume was 1 μ L, and the total run time was 10 min. The mobile phase A was composed of 10 mM ammonium formate and 0.2% formic acid in water, while mobile phase B was composed of 10 mM ammonium formate and 0.2% formic acid in 90% acetonitrile. Analytes were separated via the following gradient: held at 40% B for 2 min, linearly increased from 40% B to 90% B in 4 min, held at 90% B for 1 min, linearly decreased from 90% B to 40% B in 0.1 min, and held at 40% B for 2.9 min. MS experiments were conducted in multiple reaction monitoring (MRM) mode using an ESI ion source under positive ionization mode ($[M + H]^+$). The primary MRM transition for ergothioneine quantification was 230.2 \rightarrow 127.2, with additional transitions for qualification. Calibration was performed using a standard curve of ergothioneine (Aladdin, L134175-250 mg) ranging from 0 to 4,000 ng/mL. Data acquisition and analysis was carried out using Analyst 1.7.1 MultiQuant 3.0.3 (AB SCIEX).

Data, Materials, and Software Availability. The transcriptome sequencing data are available in the NCBI Sequence Read Archive (SRA) under Accession No. PRJNA743899 (55) and PRJNA1250935 (56) (short-term blue light responses

in *T. guizhouense*), PRJNA1184988 (57) and PRJNA1251873 (58) (constant blue light responses in *T. guizhouense*), and PRJNA1182965 (59) (red- and far-red-light responses in *A. nidulans*). This paper does not report original code. Any additional information required to reanalyze the data reported in this paper is available from the lead contact upon request. All other data are included in the manuscript and/or supporting information.

ACKNOWLEDGMENTS. This work was supported by the National Key Research and Development Program of China (Grant No. 2024YFD1700700), the National Natural Science Foundation of China (NSFC) (Grant No. 32270053 and 32402684), the Outstanding Youth Foundation of Jiangsu Province (Grant No. BK20240091), the Natural Science Foundation of Jiangsu Province (Grant No. BK20241554), the Outstanding Postdoctoral Program of Jiangsu Province (Grant No. 2024ZB328), the China Postdoctoral Science Foundation (Grant No. 2024M751441), and the Postdoctoral Fellowship Program of China Postdoctoral Science Foundation (Grant No. GZC20240711).

1. T. W. Nilsen, B. R. Graveley, Expansion of the eukaryotic proteome by alternative splicing. *Nature* **463**, 457–463 (2010).
2. A. R. Kornblihtt *et al.*, Alternative splicing: A pivotal step between eukaryotic transcription and translation. *Nat. Rev. Mol. Cell Biol.* **14**, 153–165 (2013).
3. X. Yang *et al.*, Widespread expansion of protein interaction capabilities by alternative splicing. *Cell* **164**, 805–817 (2016).
4. Y. Shi, Mechanistic insights into precursor messenger RNA splicing by the spliceosome. *Nat. Rev. Mol. Cell Biol.* **18**, 655–670 (2017).
5. L. E. Marasco, A. R. Kornblihtt, The physiology of alternative splicing. *Nat. Rev. Mol. Cell Biol.* **24**, 242–254 (2023).
6. J. Sales-Lee *et al.*, Coupling of spliceosome complexity to intron diversity. *Curr. Biol.* **31**, 4898–4910 (2021).
7. E. Boel *et al.*, Glucoamylases G1 and G2 from *Aspergillus niger* are synthesized from two different but closely related mRNAs. *EMBO J.* **3**, 1097–1102 (1984).
8. S. Fang *et al.*, The occurrence and function of alternative splicing in fungi. *Fungal Biol. Rev.* **34**, 178–188 (2020).
9. K. Grutzmann *et al.*, Fungal alternative splicing is associated with multicellular complexity and virulence: A genome-wide multi-species study. *DNA Res.* **21**, 27–39 (2014).
10. G. Janbon, Introns in *Cryptococcus*. *Mem. Inst. Oswaldo Cruz.* **113**, e170519 (2018).
11. M. Wang *et al.*, The RNA binding protein FgRbp1 regulates specific pre-mRNA splicing via interacting with U2AF23 in *Fusarium*. *Nat. Commun.* **12**, 2661 (2021).
12. J. Freitag, J. Ast, M. Bölker, Cryptic peroxisomal targeting via alternative splicing and stop codon read-through in fungi. *Nature* **485**, 522–525 (2012).
13. S. Muzafar *et al.*, Identification of genomewide alternative splicing events in sequential, isogenic clinical isolates of *Candida albicans* reveals a novel mechanism of drug resistance and tolerance to cellular stresses. *mSphere* **5**, e00608 (2020).
14. R. Betz *et al.*, Alternative splicing regulation in plants by SP7-like effectors from symbiotic arbuscular mycorrhizal fungi. *Nat. Commun.* **15**, 7107 (2024).
15. L. M. Corrochano, Light in the fungal world: From photoreception to gene transcription and beyond. *Annu. Rev. Genet.* **53**, 149–170 (2019).
16. Z. Yu, R. Fischer, Light sensing and responses in fungi. *Nat. Rev. Microbiol.* **17**, 25–36 (2019).
17. A. Blumenstein *et al.*, The *Aspergillus nidulans* phytochrome FphA represses sexual development in red light. *Curr. Biol.* **15**, 1833–1838 (2005).
18. Z. Yu, O. Armant, R. Fischer, Fungi use the Saka (HogA) pathway for phytochrome-dependent light signalling. *Nat. Microbiol.* **1**, 16019 (2016).
19. Y. Li *et al.*, Comprehensive analysis of the regulatory network of blue-light-regulated conidiation and hydrophobin production in *Trichoderma guizhouense*. *Environ. Microbiol.* **23**, 6241–6256 (2021).
20. H. Shikata *et al.*, Phytochrome controls alternative splicing to mediate light responses in *Arabidopsis*. *Proc. Natl. Acad. Sci. U.S.A.* **111**, 18781–18786 (2014).
21. C. Wu *et al.*, Genome-wide characterization of light-regulated genes in *Neurospora crassa*. *G3 (Bethesda)* **4**, 1731–1745 (2014).
22. Z. Yu *et al.*, Genome-wide analyses of light-regulated genes in *Aspergillus nidulans* reveal a complex interplay between different photoreceptors and novel photoreceptor functions. *PLoS Genet.* **17**, e1009845 (2021).
23. L. Chen, L. Zhang, X. Ye, Z. Deng, C. Zhao, Ergothioneine and its congeners: anti-ageing mechanisms and pharmacophore biosynthesis. *Protein Cell* **15**, 191–206 (2024).
24. M. H. Bello, V. Barrera-Perez, D. Morin, L. Epstein, The *Neurospora crassa* mutant Δ *NcEgt-1* identifies an ergothioneine biosynthetic gene and demonstrates that ergothioneine enhances conidial survival and protects against peroxide toxicity during conidial germination. *Fungal Genet. Biol.* **49**, 160–172 (2012).
25. Y. Li *et al.*, A simple and low-cost strategy to improve conidial yield and stress resistance of *Trichoderma guizhouense* through optimizing illumination conditions. *J. Fungi* **8**, 50 (2022).
26. R. Jaimés-Arroyo *et al.*, The SrkA kinase is part of the Saka (HogA) pathway for phytochrome-dependent light signalling and regulates stress responses and development in *Aspergillus nidulans*. *Eukaryot. Cell* **14**, 495–510 (2015).
27. W. Shi *et al.*, The rice blast fungus SR protein 1 regulates alternative splicing with unique mechanisms. *PLoS Pathog.* **18**, e1011036 (2022).
28. F. Lara-Rojas, O. Sanchez, L. Kawasaki, J. Aguirre, *Aspergillus nidulans* transcription factor AtfA interacts with the MAPK Saka to regulate general stress responses, development and spore functions. *Mol. Microbiol.* **80**, 436–454 (2011).
29. T. Sun *et al.*, Red and far-red light improve the antagonistic ability of *Trichoderma guizhouense* against phytopathogenic fungi by promoting phytochrome-dependent aerial hyphal growth. *PLoS Genet.* **20**, e1011282 (2024).
30. A. Diernfellner *et al.*, Long and short isoforms of *Neurospora* clock protein FRQ support temperature-compensated circadian rhythms. *FEBS Lett.* **581**, 5759–5764 (2007).
31. D. Ye, C. H. Lee, S. F. Queener, Differential splicing of *Pneumocystis carinii* f. sp. *carinii* inosine 5'-monophosphate dehydrogenase pre-mRNA. *Gene* **263**, 151–158 (2001).
32. N. S. Mendes *et al.*, Transcriptome-wide survey of gene expression changes and alternative splicing in *Trichophyton rubrum* in response to undecanoic acid. *Sci. Rep.* **8**, 2520 (2018).
33. J. Purschwitz *et al.*, Functional and physical interaction of blue- and red-light sensors in *Aspergillus nidulans*. *Curr. Biol.* **18**, 255–259 (2008).
34. M. S. Sachs, C. Yanofsky, Developmental expression of genes involved in conidiation and amino acid biosynthesis in *Neurospora crassa*. *Dev. Biol.* **148**, 117–128 (1991).
35. E. Mancini *et al.*, Acute effects of light on alternative splicing in light-grown plants. *Photochem. Photobiol.* **92**, 126–133 (2016).
36. E. Petrillo *et al.*, A chloroplast retrograde signal regulates nuclear alternative splicing. *Science* **344**, 427–430 (2014).
37. M. A. Godoy Herz *et al.*, Light regulates plant alternative splicing through the control of transcriptional elongation. *Mol. Cell* **73**, 1066–1074.e1063 (2019).
38. S. Riegler *et al.*, Light regulates alternative splicing outcomes via the TOR kinase pathway. *Cell Rep.* **36**, 109676 (2021).
39. J. L. Mateos *et al.*, P1CLN modulates alternative splicing and light/temperature responses in plants. *Plant Physiol.* **191**, 1036–1051 (2023).
40. M. Teige, E. Scheikl, V. Reiser, H. Ruis, G. Ammerer, Rck2, a member of the calmodulin-protein kinase family, links protein synthesis to high osmolarity MAP kinase signaling in budding yeast. *Proc. Natl. Acad. Sci. U.S.A.* **98**, 5625–5630 (2001).
41. E. Bisland, C. Molin, S. Swaminathan, A. Ramne, P. Sunnerhagen, Rck1 and Rck2 MAPKAP kinases and the HOG pathway are required for oxidative stress resistance. *Mol. Microbiol.* **53**, 1743–1756 (2004).
42. P. Thakran *et al.*, Sde2 is an intron-specific pre-mRNA splicing regulator activated by ubiquitin-like processing. *EMBO J.* **37**, 89–101 (2018).
43. Z. Li *et al.*, Arginine methylation is required for remodelling pre-mRNA splicing and induction of autophagy in rice blast fungus. *New Phytol.* **225**, 413–429 (2020).
44. R. Liu *et al.*, PRMT5 regulates the polysaccharide content by controlling the splicing of thaumatin-like protein in *Ganoderma lucidum*. *Microbiol. Spectr.* **11**, e0290623 (2023).
45. P. R. Birch, P. F. Sims, P. Broda, Substrate-dependent differential splicing of introns in the regions encoding the cellulose binding domains of two exocellulohydrolase I-like genes in *Phanerochaete chrysosporium*. *Appl. Environ. Microbiol.* **61**, 3741–3744 (1995).
46. Y. Baba, A. Shimonaka, J. Koga, H. Kubota, T. Kono, Alternative splicing produces two endoglucanases with one or two carbohydrate-binding modules in *Mucor circinelloides*. *J. Bacteriol.* **187**, 3045–3051 (2005).
47. S. Lawrinowitz *et al.*, Blue light-dependent pre-mRNA splicing controls pigment biosynthesis in the mushroom *Terana caerulea*. *Microbiol. Spectr.* **10**, e0106522 (2022).
48. Z. Chen *et al.*, Toward more efficient ergothioneine production using the fungal ergothioneine biosynthetic pathway. *Microb. Cell Fact.* **21**, 76 (2022).
49. V. M. Rekdal *et al.*, Edible mycelium bioengineered for enhanced nutritional value and sensory appeal using a modular synthetic biology toolkit. *Nat. Commun.* **15**, 2099 (2024).
50. F. Wang *et al.*, Transcription in fungal conidia before dormancy produces phenotypically variable conidia that maximize survival in different environments. *Nat. Microbiol.* **6**, 1066–1081 (2021).
51. E. Kafer, Meiotic and mitotic recombination in *Aspergillus* and its chromosomal aberrations. *Adv. Genet.* **19**, 33–131 (1977).
52. J. Zhang *et al.*, Guttation capsules containing hydrogen peroxide: An evolutionarily conserved NADPH oxidase gains a role in wars between related fungi. *Environ. Microbiol.* **21**, 2644–2658 (2019).
53. Y. Li *et al.*, The bZIP transcription factor ATF1 regulates blue light and oxidative stress responses in *Trichoderma guizhouense*. *mLife* **2**, 365–377 (2023).
54. F. Uzbaz, U. Sezeran, L. Hartl, C. P. Kubicek, B. Seiboth, A homologous production system for *Trichoderma reesei* secreted proteins in a cellulase-free background. *Appl. Microbiol. Biotechnol.* **93**, 1601–1608 (2012).
55. Y. Li *et al.*, Identification of blue-light-regulated genes in *Trichoderma guizhouense* after short-time blue light exposure. National Center for Biotechnology Information (NCBI). <https://www.ncbi.nlm.nih.gov/bioproject/PRJNA743899>. Deposited 5 July 2021.
56. Y. Li *et al.*, Transcriptome data of *Trichoderma guizhouense* after short-time blue light exposure. National Center for Biotechnology Information (NCBI). <https://www.ncbi.nlm.nih.gov/bioproject/PRJNA1250935>. Deposited 15 April 2025.
57. Y. Li *et al.*, Transcriptome data of *Trichoderma guizhouense* after constant blue light exposure. National Center for Biotechnology Information (NCBI). <https://www.ncbi.nlm.nih.gov/bioproject/PRJNA1184988>. Deposited 12 November 2024.
58. Y. Li *et al.*, Transcriptome data of *Trichoderma guizhouense* after constant blue light exposure. National Center for Biotechnology Information (NCBI). <https://www.ncbi.nlm.nih.gov/bioproject/PRJNA1251873>. Deposited 17 April 2025.
59. Y. Li *et al.*, Transcriptome data of *Aspergillus nidulans* after red and far-red light exposure. National Center for Biotechnology Information (NCBI). <https://www.ncbi.nlm.nih.gov/bioproject/PRJNA1182965>. Deposited 7 November 2024.